Hindawi
International Journal of Antennas and Propagation
Volume 2019, Article ID 3197497, 8 pages
https://doi.org/10.1155/2019/3197497

Research Article

Antenna Element Index Modulation for Frequency Diverse Array

Gaojian Huang,[1] **Yuan Ding**,[2] **Vincent Fusco**,[3] **and Shan Ouyang**[1]

[1]*School of Information and Communications, Guilin University of Electronic Technology, Guilin 541004, China*
[2]*The Institute of Sensors, Signals and Systems (ISSS), Heriot-Watt University, Edinburgh EH14 4AS, UK*
[3]*Institute of Electronics, Communications and Information Technology (ECIT), Queen's University of Belfast, Belfast BT3 9DT, UK*

Correspondence should be addressed to Shan Ouyang; hmoysh@guet.edu.cn

Received 16 April 2019; Revised 12 July 2019; Accepted 29 August 2019; Published 22 September 2019

Academic Editor: Pierfrancesco Lombardo

In this paper, we propose a new architecture and provide performance analysis for frequency diverse array (FDA) Radar combined with the index modulation (IM) techniques. Here, the IM concept is applied upon frequency offsets in an FDA. Information is transmitted by a dynamically selected subset of antenna element indices applying predefined carrier frequency offsets, which generate different radiation patterns. It is shown that this enables the capability for simultaneous wireless communication and FDA Radar that has the range-angle coupling issue resolved.

1. Introduction

The orthogonal frequency division multiplexing subcarrier index modulation (OFDM-SIM) concept was first introduced in [1]. This novel modulation scheme creates an additional dimension in the subcarrier index domain compared with the conventional modulation techniques. Later, an upgraded transmission approach from that in [1] was proposed, namely, OFDM index modulation (OFDM-IM) [2]. Here, a bit stream is transmitted not only through modulated radio frequency (RF) carriers but also by the indices of dynamically activated OFDM subcarriers. This concept was further extended to multiple-input multiple-output (MIMO) scenarios in [3]. While in the Radar community, the frequency diverse array (FDA) technique has been rapidly developing in recent years [4–19]. In a conventional FDA, a small amount of progressive RF carrier frequency shift Δf is applied across the array elements, resulting in a range-angle dependent pattern [4–6]. This FDA beampattern feature was mathematically derived and examined through simulation in [7, 8]. And they were further studied from a design perspective using in [9, 10]. In [11, 12], the FDA was exploited to reject range dependent interference, which endows FDA potential number of important applications on Radar and navigation [13–16]. However, for Radar applications, the range of the detection target cannot be directly obtained from the beamforming output peaks due to the inherent coupling of range and angle traditionally associated with FDA. In [17], a decoupled range-angle beampattern was proposed using logarithmically increased frequency offsets with compromised beamforming performance in range domain. Square and cubic increasing frequency offsets were also developed for decoupling in [18], which, however, require a large bandwidth. In [19], an FDA Radar using two pulses with zero and nonzero frequency increments was introduced to locate targets' range-angle coordinates, but it was only for Radar sensing.

In this paper, the authors attempt to establish a link between the IM technique and FDA Radar. The proposed antenna element IM FDA transmitters are constructed for the purpose of concurrent wireless communication and Radar sensing. The paper is organized as follows. In Section 2, the proposed antenna element IM FDA transmitter architecture is first described, followed by the elaboration of its operation principle. In Section 3, the approach to address the

range-angle entanglement is introduced, leaving simulation results and discussion presented in Section 4. Finally, conclusions are drawn in Section 5.

2. Antenna Element IM FDA Transmitter

Considering a one-dimensional (1D) N-element array with uniform element spacing d, the n^{th} element is excited with a signal of frequency:

$$f_n = f_0 + n\Delta f U_{n,q}(t), \quad n = 1, 2, \ldots, N. \tag{1}$$

here, f_0 is a reference carrier frequency, and Δf is set to be several orders smaller than f_0. $U_{n,q}(t)$ refers to the on-off function in time domain of the n^{th} single-pole single-throw switch in the q^{th} symbol slot of duration T_s,

$$U_{n,q}(t) = \begin{cases} 1, & qT_s \le t \le (q+1)T_s \text{ for selected antennas,} \\ 0, & \text{otherwise for other unselected antennas.} \end{cases} \tag{2}$$

In (2), qT_s and $(q+1)T_s$ refer to the switch-on and switch-off time instants, respectively. "1" represents "on" of the switch and "0" represents "off." For one period $T(T > T_s)$, $U_{n,q}(t)$ is shown in Figure 1. Figure 2 depicts the antenna element IM FDA transmitter architecture. Information bit steam of p bits determines the indices of antenna elements whose RF carrier frequencies are shifted. The mapping between bits and antenna indices is performed by the "Index Selector" module depicted in Figure 2. Afterwards, the selected antenna element index sequences are divided into two parts, i.e., H_{J1} and H_{J2}, respectively, corresponding to a smaller and a larger number of selected antenna elements. The closing single-pole single-throw switches of S_1 and S_2 have a duration T. ϕ_n denotes the phase shift of the n^{th} RF carrier and $\phi_n = n\phi_1$.

In the proposed antenna element IM FDA transmitter, the indices of antennas with carrier frequency offsets applied are dynamically updated in each transmitted symbol period. For each bit frame of p bits, K out of N antenna elements are selected. The selected antenna indices are grouped as

$$I_G = \{i_1, \ldots, i_g, \ldots, i_G\}, \tag{3}$$

where $i_g \in \{1, 2, \ldots, N\}$ and $i_a \ne i_b$ when $a \ne b$. I_G is determined by the baseband data of p bits, indicating

$$p = \lfloor \log_2 [C(N, K)] \rfloor, \tag{4}$$

where $C(N, K)$ refers to the number of K-combinations out of a set of N elements. Generally, $K \le N$. Operator "$\cdot$" denotes integer floor function. The mapping procedures, from p bits to K-antennas with applied carrier frequency offsets, are presented as follows:

(i) The p bits are converted to a decimal number c, using

$$c = \sum_{m=0}^{p-1} 2^m V^{(m)}, \tag{5}$$

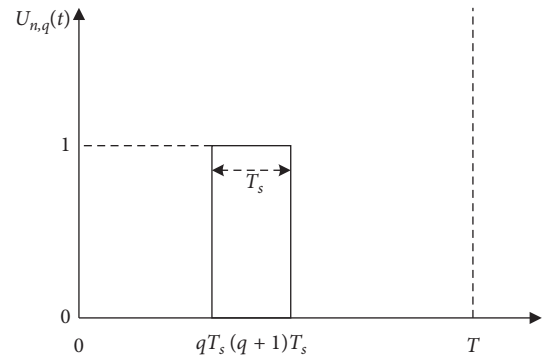

Figure 1: Illustration of on-off switch function $U_{n,q}(t)$ in time domain.

where $V^{(m)}$ denotes the m^{th} bit in the p-bit sequence D. Here, $0 \le c \le C(N, K)-1$.

(ii) Map the decimal number c to a strictly decreasing sequence $\{j_K, j_{K-1}, \ldots, j_1\}$, $j_\gamma \in \{0, 1, 2, \ldots, N-1\}$, and $j_a \ne j_b$ when $a \ne b$; j_K is the largest natural number satisfying $C(j_K, K) \le c$. In case when $c = 0$, $j_K = K - 1$. Then, j_{K-l} is the natural number satisfying

$$\begin{aligned} C(j_{K-l}, K-l) &\le c - \sum_{l=1}^{K-1} C(j_{K-l+1}, K-l+1) \\ &\le C(j_{K-l}+1, K-l). \end{aligned} \tag{6}$$

(iii) The sequence $\{j_K + 1, j_{K-1} + 1, \ldots, j_1 + 1\}$, termed as J hereafter, contains the indices of the selected antenna elements.

A one-to-one mapping between the p-bit sequences and the selected antenna indices J is guaranteed with a known K by this mapping rule [2]. To better explain the mapping procedure, a flow chart is illustrated in Figure 3. An example of $N = 16$ and $p = 6$ is discussed here. Since $p = \log_2 [C(N, k)]$, we have $K = 2$ and 14, respectively, corresponding sequence H_{J1} and H_{J2} shown in Figure 2. If we assume a p-bit (6 bit) sequence of "110001" for $K = 2$, then using (5) we get the corresponding decimal number $c = 49$. Seen from Figure 3, j_2 starts at 15, as $C(10, 2) = 45 < c = 49 < C(11, 2) = 55$; thus, 10 is the largest number that satisfies the combinational numbers smaller than c, i.e., $j_2 = 10$. Then, $c = 49 - C(10, 2) = 4$, $K = K - 1 = 1$. Similarly, via iteration, j_1 can be obtained, i.e., 4. Therefore, the sequence H_{J1} of {11, 5} contains the selected antenna indices, which uniquely represents the binary information "110001." And for $K = 14$, H_{J2} can be obtained in an analogous manner. Using H_{J1} or H_{J2} is determined by the status of the corresponding switches of S_1 and S_2. When the used element index sequence in the antenna array are known, the carrier frequency offsets are applied by closing the corresponding switches in the switch array, i.e., $U_{J,q}(t) = 1$.

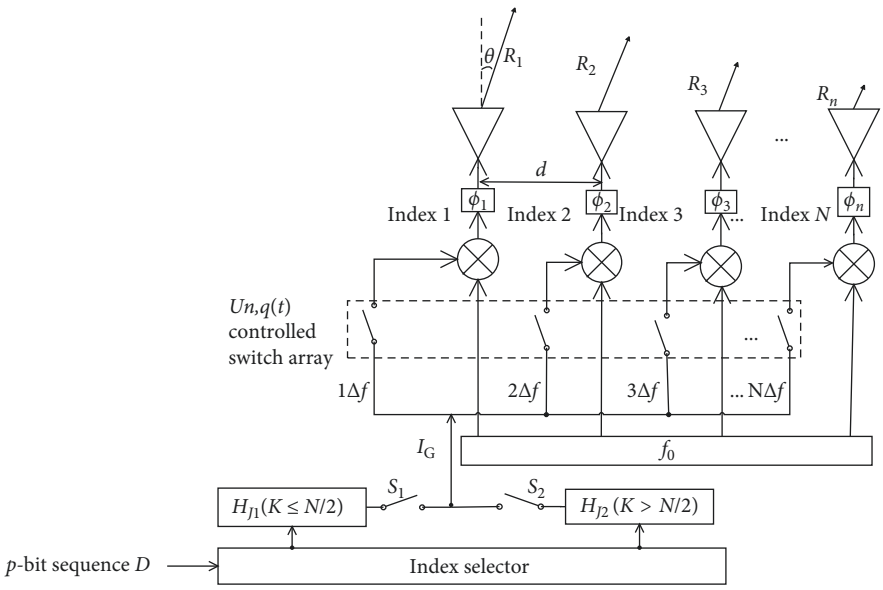

Figure 2: Architecture of proposed antenna element IM FDA transmitter.

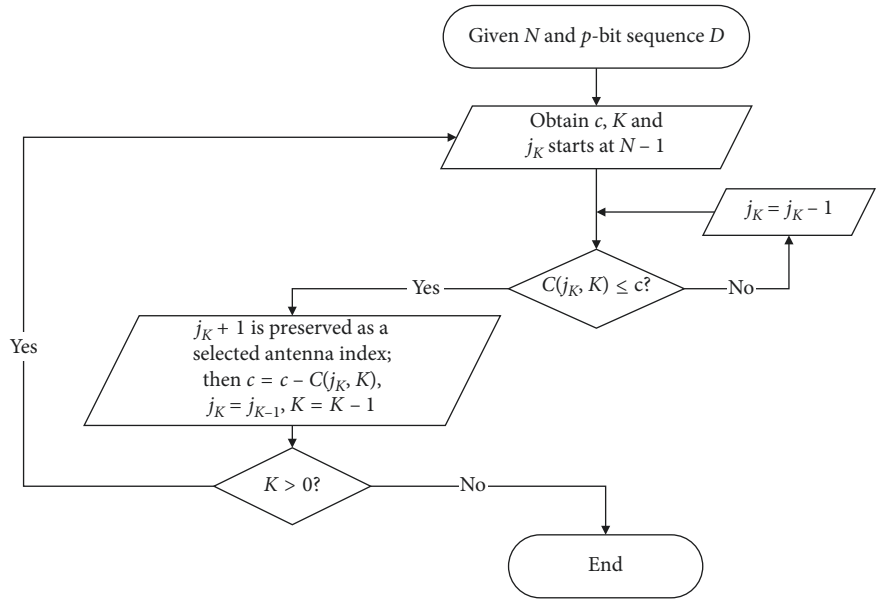

Figure 3: The flow chart of mapping procedures.

3. Resolve the Range-Angle Entanglement

In the conventional FDA (CFDA), i.e., all antenna elements are applied with their corresponding carrier frequency offsets, the radiated field in the far-field region at a location A (R_1, θ) can be expressed as

$$P(t; R_1, \theta) = \sum_{n=1}^{N} \frac{1}{R_n} \exp\left\{-j\left[2\pi\left(f_n t - \frac{R_n}{\lambda_n}\right) - \phi_n\right]\right\}, \quad 0 \le t \le T, \tag{7}$$

where T is transmitted pulse duration that is further divided into h equal subpulses of duration T_s. λ_n is the wavelength corresponding to the operation frequency f_n, i.e., $\lambda_n = c_0/f_n$, where c_0 is the speed of light. R_n is the receiver displacement in free space with respect to the n^{th} element that is given by

$$R_n = R_1 - (n-1)d \sin\theta. \tag{8}$$

θ is the spatial angle away off the array boresight. Since $(N-1)\Delta f << f_1$ and $R_n \approx R_1$, the far field pattern can be approximated as

$$P(t; R_1, \theta) \approx \frac{\exp(j\varphi)}{R_1} \frac{\sin(N\pi\Phi)}{\sin(\pi\Phi)},$$
$$\Phi = \Delta f t - \frac{\Delta f R_1}{c_0} + \frac{d f_1 \sin\theta}{c_0} + \phi_1, \tag{9}$$

where $\varphi = -2\pi f_1(t - R_1/c_0)$. The maximum values of P are obtained when

$$\Delta f t - \frac{\Delta f R_1}{c_0} + \frac{d f_1 \sin\theta}{c_0} + \phi_1 = M, \quad M = 0, 1, 2, \ldots. \tag{10}$$

From (10), it can be observed that the range and angle of far field location A are coupled when the time variable t and M are fixed. It is noted that when none of the antenna elements are selected for frequency offsets, i.e., $K = 0$, the far-field pattern becomes

$$P(t;\theta) \approx \frac{\exp(j\varphi)}{R_1} \frac{\sin\{N\pi(d f_1 \sin\theta/c_0 + \phi_1)\}}{\sin\{\pi(d f_1 \sin\theta/c_0 + \phi_1)\}}, \tag{11}$$

that is, the classical phased array (PA) beampattern. In a specific region, the coupled range-angle beampattern issue can be resolved by hybridizing the properties of a PA, and an FDA in the proposed antenna element IM FDA through setting different numbers of antenna elements with applied frequency offsets. The operation can be summarized as follows:

(1) Estimate θ by using the obtained quasi-PA beampattern. In one period of duration T, select fewer antenna elements, i.e., close the switch S_1. Meanwhile, close the switches of antenna branches with indices identified in H_{J1}. According to the mapping rules described above for the continuous p-bit streams, a beampattern which has quasi-PA characteristics is obtained to evaluate the azimuth angle θ in (10) and binary information is conveyed by the selected antenna element indices.

(2) Obtain range information from the range-angle dependant beampattern with the aid of estimated θ obtained in the first step. In another T, increase the number of selected antenna elements through opening the switch S_1 and closing the switch S_2. Also, close the switches in the switch array in accordance with H_{J2}. This operation forms a range-angle dependant beampattern with the transmitted bits. Since θ is known, R_1 in (10) can be derived.

4. Simulation Results and Analysis

To validate the efficacy of the proposed antenna element IM FDA transmitter, the radiated patterns are simulated that carrier bit streams for transmission. The parameters of the linear antenna element IM FDA transmitter used in the simulation are listed in Table 1. In a single duration T with closing the switch S_1, assume a bit sequence comprising 80 bits is to be transmitted. The bit sequence is equally divided into 20 sections, and each part has 4 bits. If assume one of the 20 sections to be "0001," and it is conveyed with $K = 1$. Using the mapping rule described earlier, the selected antenna element index sequence H_{J1} is calculated to be {2}. Then, remaining bits, as blocks of 4 bit, are transmitted in the same manner. Similarly, when assuming 120 bits to be transmitted, K is set to 2. In the next duration T, if the bit stream contains 80 bits or 120 bits, each of the divided 20 sections respectively corresponds to 15 or 14 selected antenna elements for H_{J2} as $\log_2[C(16, 15)] = 4$ bits and $\log_2[C(16, 14)] = 6$ bits. Here, the average radiation pattern of 20 (T/T_s) randomly generated shapes (each radiation pattern shape corresponds to one transmitted data symbol which is mapped upon the selected antenna element indices) is considered.

Table 1: Parameters for linear antenna element IM FDA simulation.

Parameters	Values
Number of antenna elements N	16
Reference carrier frequency f_0	8 GHz
Frequency offset Δf	3 kHz
Element spacing d	0.015 m
Transmitted pulse duration T	2 ms
One symbol duration T_s	0.1 ms

In Figure 4, the proposed antenna element IM FDA radiation patterns in the range-angle dimension are simulated for different values of K. The sample results in Figures 4(a) and 4(c) validate that the pattern characteristics of the phased array are well preserved with smaller K of antenna element IM FDA. While in Figures 4(b) and 4(d) with larger K, the "S"-shaped patterns are obtained, i.e., CFDA radiated patterns. In Figure 5, the target responses using the proposed scheme are depicted. Seen from Figure 5(a), in the angle domain, when compared with the first sidelobe level of the phased array ($K = 0$), i.e., around −13 dB, the proposed scheme ($K = 1, 2$) can achieve the same level. In addition, it is shown that similar peak of first sidelobe levels as CFDA are obtained for $K = 14, 15$ at a fixed range. While in the range domain, Figure 5(b) shows that the same peak-to-sidelobe ratios (PSLs) can be achieved in the proposed scheme by comparison with the CFDA scheme. It is noted that for $K = 14$, the sidelobe levels are higher. This is because that with decreased number K, a PA radiation pattern characteristic at the sidelobe level about −18 dB at 50 km range occurs, see Figure 4(d). Meanwhile, in Figure 4(c), the characteristics of CFDA radiation pattern occur at low energy level with increasing K. These features are validated in Figure 6. When $K \leq 8$, a PA radiation pattern is dominated, and the peak of first sidelobes are directly proportional to the selected K, indicating that the characteristics of the CFDA pattern are becoming obvious with increased K, and when $K > 8$, a CFDA radiation pattern is dominated. Hence, to achieve better PSLs, only smaller K and larger K are selected in the proposed scheme. This selected value of K also affects the bit rate which is described in Figure 7, showing that a trade-off exists between Radar detection performance and communication bit rate when N is fixed. In Figure 8, the range and angle of the target locations are estimated by the proposed scheme using the multiple signal classification (MUSIC) algorithm. In Figure 8(a), integrating two settings of $K_1 = 1$ and $K_2 = 15$, at the direction $\theta = 30^\circ$, two target locations that 5 km away from each other can be identified in range domain. And these two ranges can also be successfully estimated with setting $K_1 = 2$ and $K_2 = 14$ at the direction $\theta = 60^\circ$, shown in Figure 8(b). Figures 9(a)–9(c)

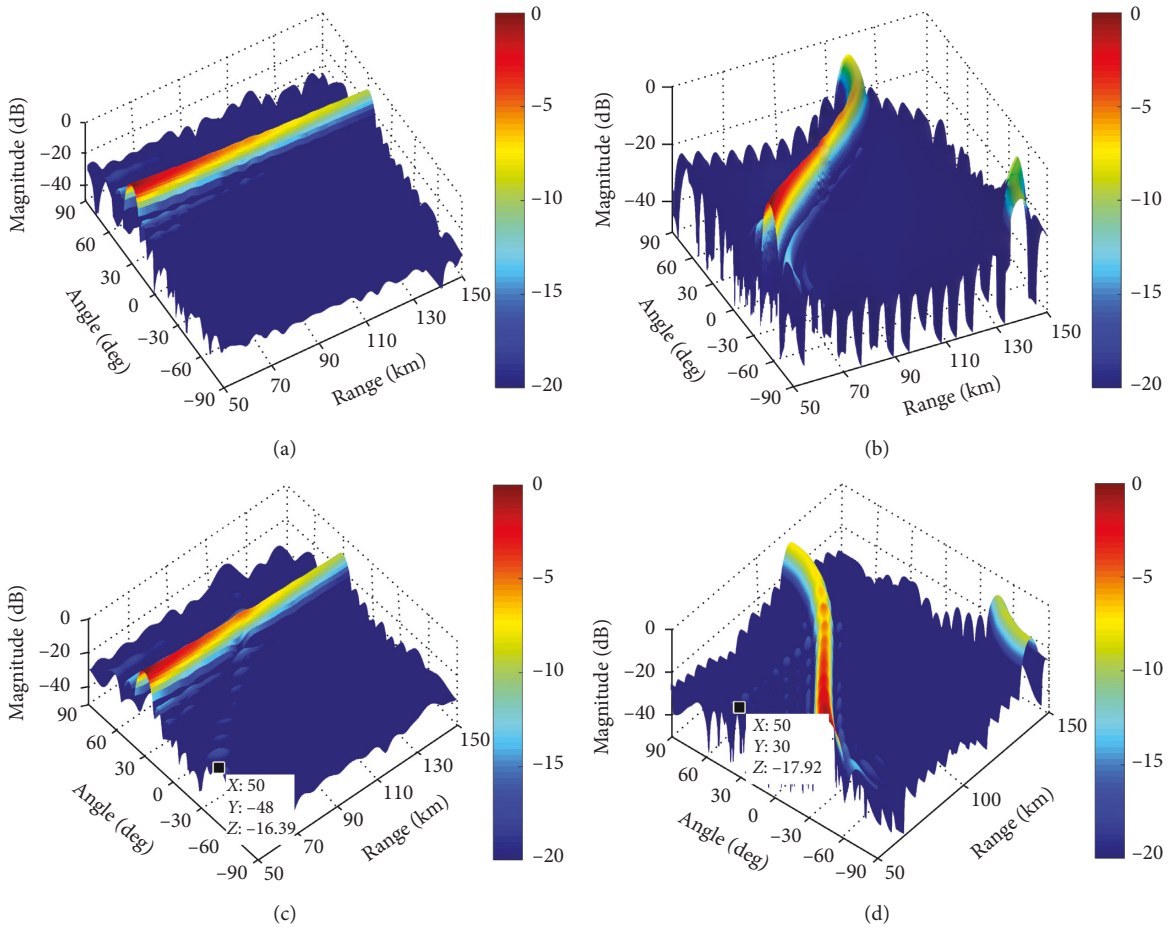

FIGURE 4: Snapshots of one-way normalised radiation pattern at $t = 4/\Delta f$, $\theta = 30^\circ$ for (a) $K_1 = 1$, (b) $K_2 = 15$, (c) $K_1 = 2$, and (d) $K_2 = 14$.

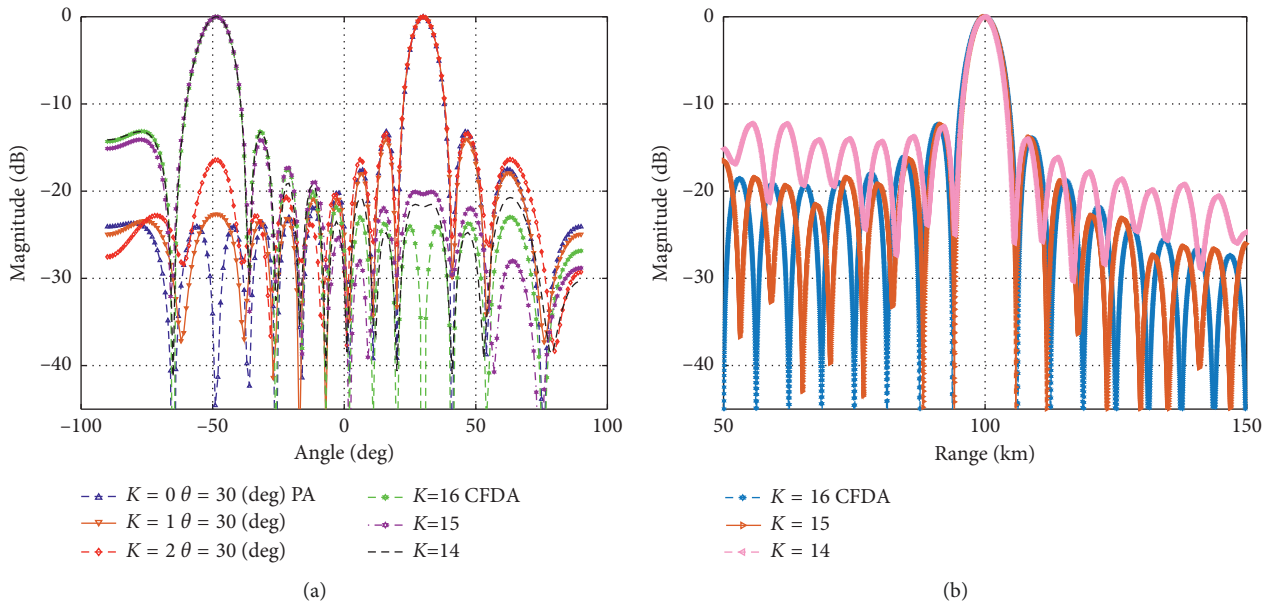

FIGURE 5: Target responses when $\theta = 30^\circ$, $t = 4/\Delta f$ for (a) the angle profile when $R_1 = 50$ km and (b) the range profile.

compare the MUSIC spectra of target 3 and target 4 using the proposed antenna element FDA with those FDAs employing square, cubic and logarithmically increasing frequency offsets, respectively. It can be seen from Figures 9(a) and 9(b) that the two targets can be detected along with some other fake targets. Therefore, target

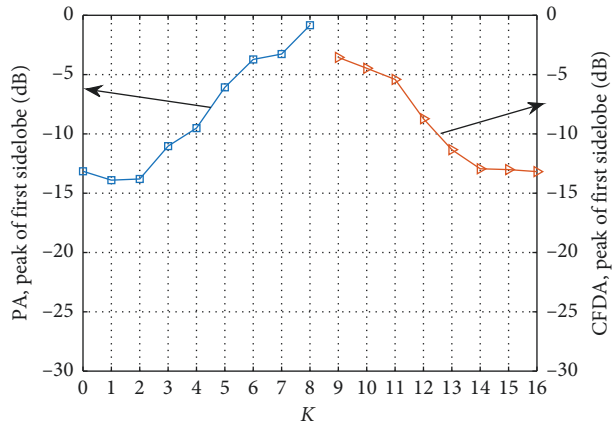

Figure 6: Peak of first sidelobe levels of the dominated PA and CFDA pattern, respectively, corresponds to $K \leq 8$ and $K > 8$, with $N = 16$ and $R_1 = 50$ km.

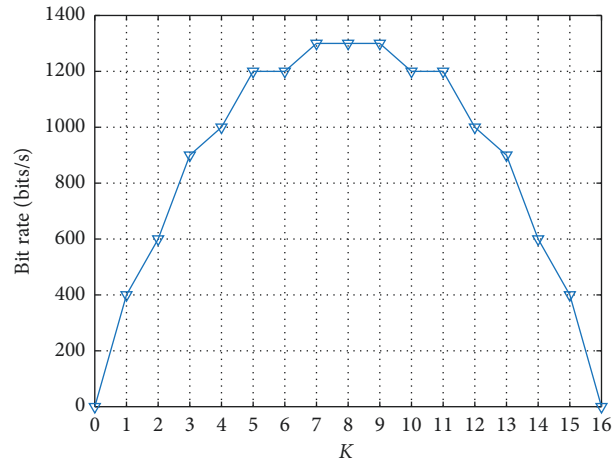

Figure 7: Bit rate of the proposed scheme for various K with $N = 16$, $\Delta f = 3$ kHz, and $T_s = 0.1$ ms.

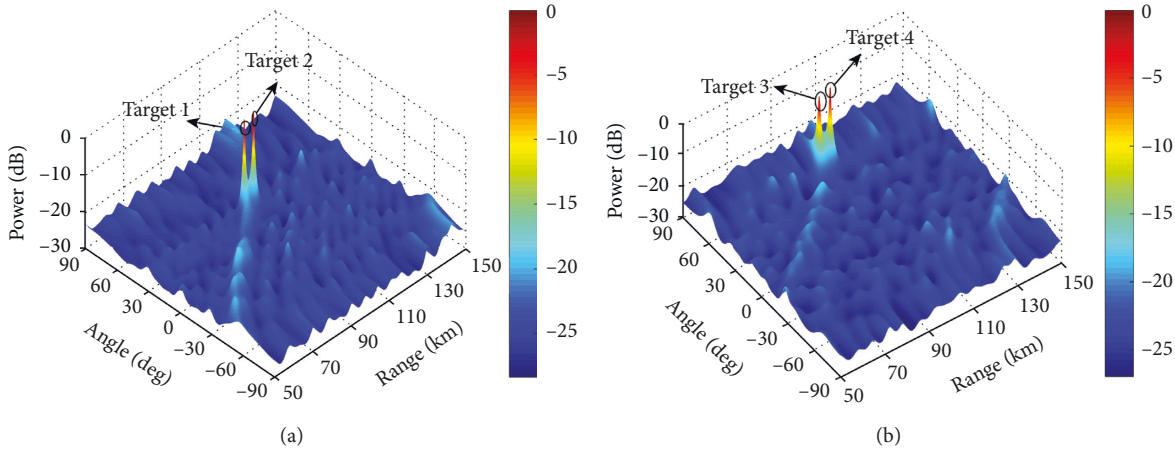

Figure 8: MUSIC spectra by using the proposed scheme for (a) target 1 (100 km, 30°) and target 2 (105 km, 30°) with $K_1 = 1$ and $K_2 = 15$ and (b) target 3 (100 km, 60°) and target 4 (105 km, 60°) with $K_1 = 2$ and $K_2 = 14$.

ambiguity problem exists. This is can be explained that the square and cubic frequency offset FDA beampatterns have multiple maxima peaks in the range domain, and the larger bandwidth results in a shorter distance among the peaks. In Figure 9(c), it is shown that targets 3 and 4 cannot be separated in the range domain by the log-FDA scheme

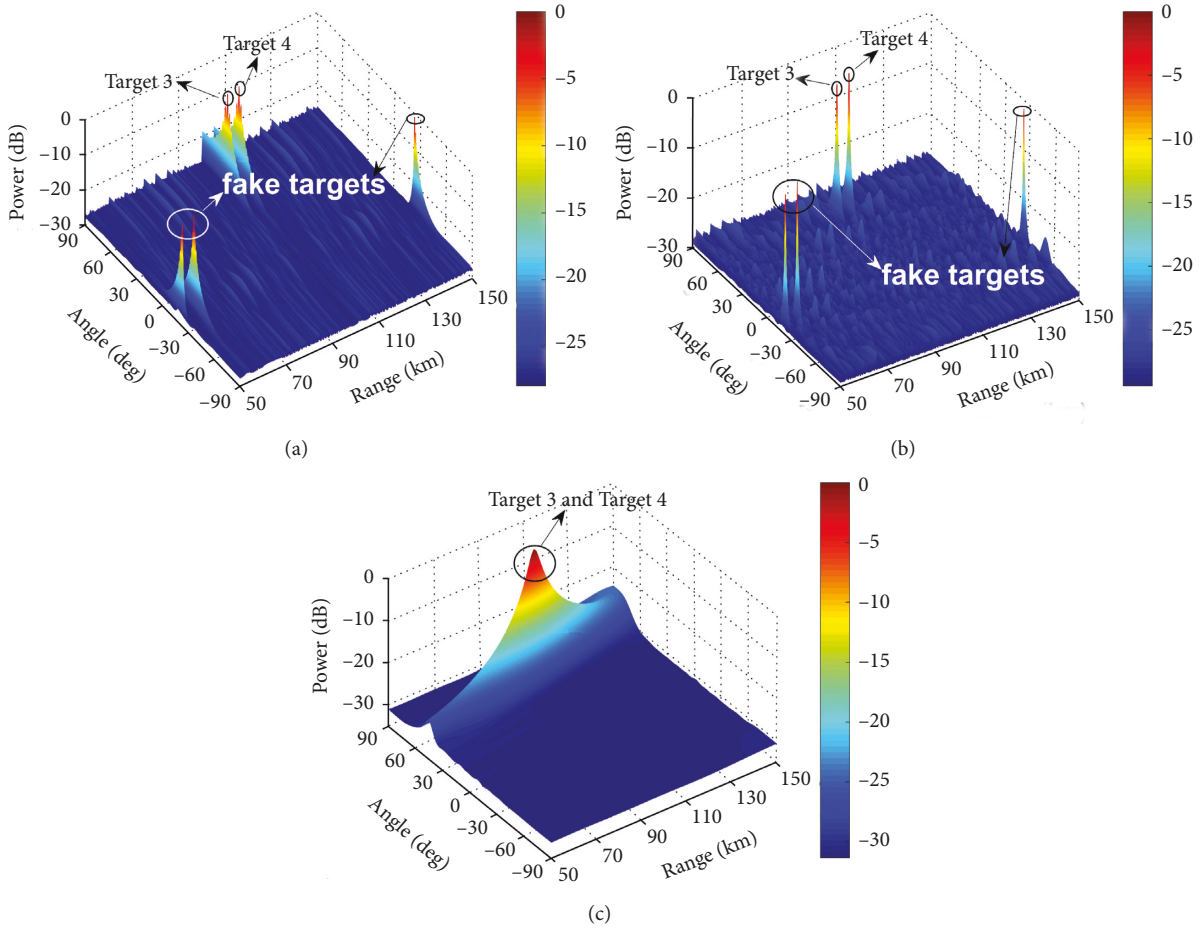

FIGURE 9: Comparisons of MUSIC spectra of target 3 and target 4 for (a) square increasing frequency offset FDA with $M = 16$, $\Delta f = 3$ kHz [18]; (b) cubic increasing frequency offset FDA with $M = 16$, $\Delta f = 3$ kHz [18]; and (c) log-increasing frequency offset FDA (log-FDA) with $M = 16$, $\delta = 3$ kHz [17].

because of the compromised resolution in the range domain.

5. Conclusions

Inspired by the IM concept, an antenna element IM FDA transmitter was proposed that has the ability to simultaneously deliver data wirelessly and Radar sensing. Also, the inherent range-angle coupling issue associated with an FDA system can be addressed in a specific area by varying the number of antenna elements with applied frequency offsets. The proposed transmission scheme can be further extended with the support of experimental verification in the indoor environment. This is planned in the near future. The phase-locked loop (PLL) frequency synthesizers sharing the same reference signal are considered to be fit for FDA frequency generations. This antenna element IM FDA transmitter concept introduced in the paper should be useful in applications where there is a need for a communication link in addition to the Radar sensing.

Data Availability

No data were used to support this study.

Conflicts of Interest

The authors declare that there are no conflicts of interest regarding the publication of this paper.

Acknowledgments

This work was supported by the National Natural Science Foundation of China under Grant no.61871425, the Study Abroad Program for Graduate Student from Guilin University of Electronic Technology (GUET), China, and the Innovation Project of GUET Graduate Education.

References

[1] R. Abu-Alhiga and H. Haas, "Subcarrier-index modulation OFDM," in *Proceedings of the IEEE 20th International Symposium on Personal, Indoor and Mobile Radio Communications*, pp. 177–181, Tokyo, Japan, September 2009.

[2] E. Basar, U. Aygolu, E. Panayirci, and H. V. Poor, "Orthogonal frequency division multiplexing with index modulation," *IEEE Transactions on Signal Processing*, vol. 61, no. 22, pp. 5536–5549, 2013.

[3] E. Basar, "On multiple-input multiple-output OFDM with index modulation for next generation wireless networks,"

IEEE Transactions on Signal Processing, vol. 64, no. 15, pp. 3868–3878, 2016.

[4] P. Antonik, M. C. Wicks, H. D. Griffiths, and C. J. Baker, "Frequency diverse array radars," in *Proceedings of the IEEE Conference on Radar*, pp. 215–217, Verona, NY, USA, February 2006.

[5] P. Antonik, M. C. Wicks, H. D. Griffiths, and C. J. Baker, "Range-dependent beamforming using element level waveform diversity," in *Proceedings of the International Waveform Diversity & Design Conference*, pp. 1–6, Lihue, HI, USA, January 2006.

[6] P. Antonik, *An investigation of a frequency diverse array*, Ph.D. Dissertation, University College London, London, UK, 2009.

[7] M. Secmen, S. Demir, A. Hizal, and T. Eker, "Frequency diverse array antenna with periodic time modulated pattern in range and angle," in *Proceedings of the IEEE Radar Conference*, pp. 427–430, Boston, MA, USA, May 2007.

[8] W.-Q. Wang, H. Shao, and J. Y. Cai, "A flexible phased-MIMO array antenna with transmit beamforming," *International Journal of Antennas and Propagation*, vol. 2012, pp. 1–10, 2012.

[9] J. Huang, K. Tong, and C. J. Baker, "Frequency diverse array with beam scanning feature," in *Proceedings of the IEEE Antennas and Propagation Society International Symposium*, pp. 1–4, San Diego, CA, USA, July 2008.

[10] J. Huang, K. Tong, and C. Baker, "Frequency diverse array: simulation and design," in *Proceedings of the Loughborough Antennas & Propagation Conference*, pp. 253–256, Loughborough, UK, November 2009.

[11] P. Baizert, T. B. Hale, M. A. Temple, and M. C. Wicks, "Forward-looking radar GMTI benefits using a linear frequency diverse array," *Electronics Letters*, vol. 42, no. 22, pp. 1311-1312, 2006.

[12] P. Baizert, "Forward-looking radar clutter suppression using frequency diverse arrays," Master's thesis, Air Force Institute of Technology, Dayton, OH, USA, 2006.

[13] J. Farooq, M. A. Temple, and M. A. Saville, "Application of frequency diverse arrays to synthetic aperture radar imaging," in *Proceedings of the International Conference on Electromagnetics in Advanced Applications*, pp. 447–449, Torino, Italy, September 2007.

[14] J. Farooq, M. A. Temple, and M. A. Saville, "Exploiting frequency diverse array processing to improve SAR image resolution," in *Proceedings of the IEEE Radar Conference*, pp. 1–5, Rome, Italy, May 2008.

[15] W. Wang and H. C. So, "Transmit subaperturing for range and angle estimation in frequency diverse array radar," *IEEE Transactions on Signal Processing*, vol. 62, no. 8, pp. 2000–2011, 2014.

[16] W. Wang, "Frequency diverse array antenna: new opportunities," *IEEE Antennas and Propagation Magazine*, vol. 57, no. 2, pp. 145–152, 2015.

[17] W. Khan, I. M. Qureshi, and S. Saeed, "Frequency diverse array radar with logarithmically increasing frequency offset," *IEEE Antennas and Wireless Propagation Letters*, vol. 14, pp. 499–502, 2015.

[18] K. Gao, W. Wang, J. Cai, and J. Xiong, "Decoupled frequency diverse array range-angle-dependent beampattern synthesis using non-linearly increasing frequency offsets," *IET Microwaves, Antennas and Propagation*, vol. 10, no. 8, pp. 880–884, 2016.

[19] W. Wang and H. Shao, "Range-angle localization of targets by a double-pulse frequency diverse array radar," *IEEE Journal of Selected Topics in Signal Processing*, vol. 8, no. 1, pp. 106–114, 2014.